Electronic Supplementary Material (ESI) for RSC Advances.

Supplementary Information

Layered mesoporous $Mg(OH)_2$/GO nanosheet composite for efficient removal of water contaminants

Panpan Wang [a], Yixing Ye [a], Dewei Liang [a, b], Hongmei Sun [a, b], Jun Liu [a], Zhenfei Tian [a] and Changhao Liang [a, b*]

[a]*Key Laboratory of Materials Physics and Anhui Key Laboratory of Nanomaterials and Nanotechnology, Institute of Solid State Physics, Chinese Academy of Sciences, Hefei 230031, China.*

[b]*Department of Materials Science and Engineering, University of Science and Technology of China, Hefei 230026,China.*

*Corresponding author. Tel.: +86 551 65591129; Fax: +86 551 65591434.

E-mail address: chliang@issp.ac.cn (C. H. Liang).

Digital pictures of GO synthesized by Hummers' method and colloid after laser ablated were shown in Figure S1. $Mg(OH)_2$ and $Mg(OH)_2$/GO composite colloids were both turbid compared with transparent GO solution. $Mg(OH)_2$ turns to be turbid because of the nanoflakes nature of $Mg(OH)_2$, but the reason of $Mg(OH)_2$/GO composite colloids become cloudy is electrostatic interaction between positively charged and negatively charged GO. Figure S2 shows the hexagonal stack morphology and XRD pattern of $Mg(OH)_2$ nanoflakes. All peaks coincide with PDF No. 00-44-1482, except that the strongest peak is not (101) but (001) and all peaks shows non-uniform broadening, which is caused by various disorders, such as stack faults or interstratifications in layered materials.[1] It is obvious that MB is a cationic dye from the MB molecular structure, as shown in Figure S3. Digital pictures of MB solution after different contact time were shown in Figure S4. And the color becomes lighter gradually. Table S1-S4 shows pseudo-second-order model adsorption kinetics constants, intro-particle diffusion model constants, equilibrium adsorption isotherm fitting parameters, and specific data of heavy metal ions adsorption respectively.

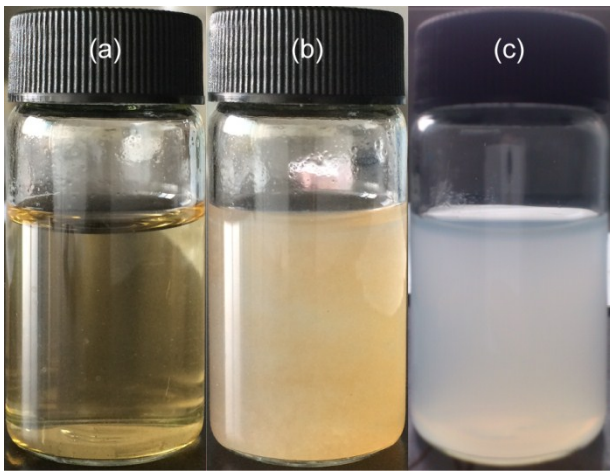

Figure S1. Digital pictures of (a) GO solution, (b) as-prepared $Mg(OH)_2$/GO composite, (c) pure $Mg(OH)_2$.

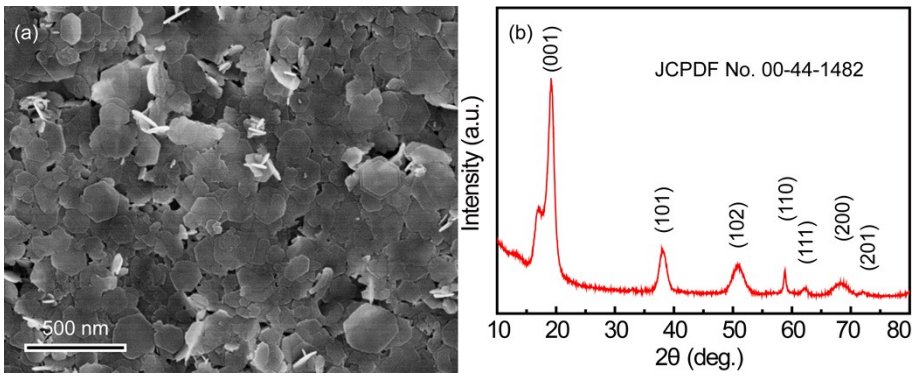

Figure S2. SEM morphology and XRD pattern of the pure $Mg(OH)_2$ nanoflakes.

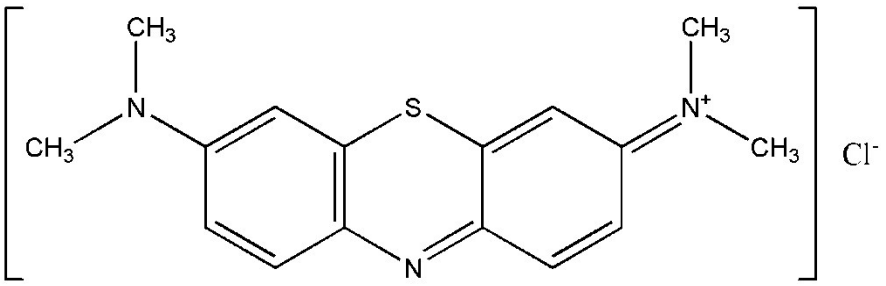

Figure S3. The molecule structure of MB

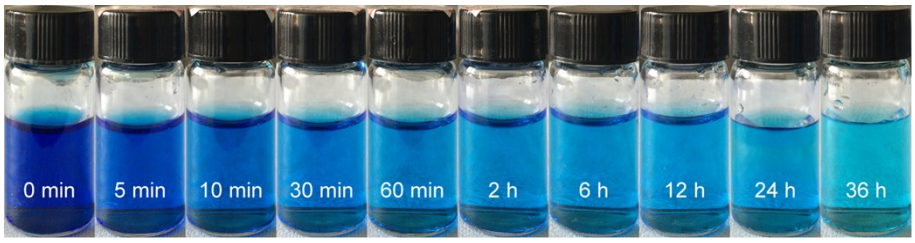

Figure S4. Digital pictures for the MB solution (100 mg L^{-1}, 20mL) and those after treatment with $Mg(OH)_2$/GO composite (20mg) at different time.

Table S1. Pseudo-second-order model adsorption kinetics constants

$q_{e,exp}$ (mg g^{-1})	$q_{e,cal}$ (mg g^{-1})	k_2 ($\times 10^{-4}$ g mg^{-1} min^{-1})	V_0 (g mg^{-1} min^{-1})	R^2
88.2	87.7	3.88	2.99	0.998

Table S2. Intro-particle diffusion model constants and correlation coefficients

	k_{di} (mg g^{-1} $min^{-1/2}$)	C_i	R^2
Stage 1	12.07	18.03	1
Stage 2	2.03	50.95	0.940
Stage 3	0.49	65.3	0.967

Table S3. Equilibrium adsorption isotherm fitting parameters

Linear fitting			
Langmuir isotherm	q_m (mg g-1)	k_L (L mg^{-1})	R^2
	555.6	0.00966	0.967
Freundlich isotherm	1/n	k_F	R^2
	0.36	39.8	0.993
Non-linear fitting			
Langmuir isotherm	q_m (mg g-1)	k_L (L mg^{-1})	R^2
	609.5	0.0048	0.967
Freundlich isotherm	1/n	k_F	R^2
	0.39	34.2	0.992

Table S4. Equilibrium adsorption capacity and removal efficiency data of heavy metal ion adsorbed by $Mg(OH)_2$/GO nanoflowers

Metal species	Zn^{2+}	Pb^{2+}	Cu^{2+}	Ni^{2+}
Equilibrium adsorption capacities (mg g^{-1})	327.7	344.4	215.5	174.7
Removal capacity (%)	99.9	99.6	62.1	57.2

Reference

1 Liang, Changhao, et al. Pulsed-laser ablation of Mg in liquids: surfactant-directing nanoparticle assembly for magnesium hydroxide nanostructures. Chemical Physics Letters 389.1 (2004): 58-63.